Interfaces

DOI: 10.1002/anie.200701609

$\chi^{(4)}$ Raman Spectroscopy for Buried Water Interfaces

*Shoichi Yamaguchi and Tahei Tahara**

Water interfaces buried in condensed media play very important roles in a number of scientific fields, ranging from industrial chemistry to molecular biology.[1] For example, solid/water interfaces are directly involved in electrode reactions and catalytic reactions. Interest in liquid/liquid interfaces is largely concerned with emulsions and foams, which are essential in environmental and food sciences. In biological systems, we can see rich interfacial phenomena such as selective permeability and molecular recognition by cell membranes. The scientific significance of such buried interfaces has stimulated many theoretical and experimental studies.

Infrared-visible vibrational sum frequency generation (VSFG) spectroscopy, which takes advantage of the interface selectivity of $\chi^{(2)}$ (the *n*th-order nonlinear optical susceptibility is written as $\chi^{(n)}$), has been widely used to investigate liquid interfaces.[1–6] VSFG is now an indispensable tool for studying interfaces, and especially the interfacial molecular structure of water has been intensively discussed on the basis of VSFG data. Nevertheless, for buried interfaces, the applicability of VSFG is limited to some specific cases, because an IR input beam cannot reach interfaces sandwiched by most common liquids and solids, which have very strong absorption in the IR region. Therefore, experimental research on solute molecules at buried water interfaces has remained unexplored because of a lack of suitable probing techniques, although solute molecules are vitally important in many interfacial phenomena.

Herein we report a novel interface-selective fourth-order nonlinear ($\chi^{(4)}$) Raman spectroscopy that can provide heterodyne-detected vibrational spectra of interfacial solute molecules for the whole fingerprint region. The most significant advantage of this method is that it can be applied to buried interfaces, because it utilizes only visible or near-IR light. We have applied this technique to probe a dye molecule, namely, rhodamine 800 (R800, Figure 1a), at the air/water and fused silica/water interfaces. The $\chi^{(4)}$ Raman spectra of R800 at the interfaces indicated the existence of interface-specific H-bonds that have never been found in the bulk.

The $\chi^{(4)}$ Raman spectroscopy is technically built on the $\chi^{(2)}$ electronic sum frequency generation (ESFG) recently reported by us.[7] Figure 1b shows the energy diagram of ESFG. An interface is irradiated by ω_1 (narrow-band) and ω_2 (broadband) femtosecond pulses, and the ESFG signal of $\omega_1+\omega_2$ generated at the interface is detected in a multiplex way. Because the ω_1 and ω_2 pulses consist of visible or near-IR light, the ESFG spectrum represents interfacial electronic structure, instead of the vibrational structure that is conventionally observed by VSFG measurements. The energy diagram of $\chi^{(4)}$ Raman spectroscopy is shown in Figure 1c. As indicated by the left two arrows, the difference frequency of the ω_2 and ω_1 pulses is in resonance with a vibrational level

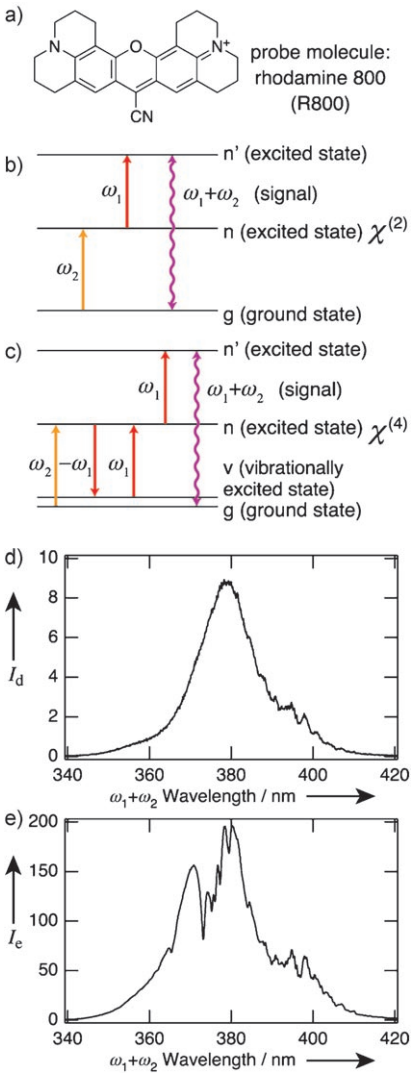

Figure 1. a) Molecular structure of rhodamine 800 (R800). b) Energy diagram of $\chi^{(2)}$ ESFG spectroscopy. c) Energy diagram of $\chi^{(4)}$ Raman spectroscopy. d) and e) ESFG spectra of R800 at the air/water interface obtained with ω_1 pulse energies of 0.7 μJ and 25 μJ, respectively. See the Supporting Information for experimental details.

[*] Dr. S. Yamaguchi, Dr. T. Tahara
Molecular Spectroscopy Laboratory
RIKEN (The Institute of Physical and Chemical Research)
2-1 Hirosawa, Wako 351-0198 (Japan)
Fax: (+81) 48-467-4539
E-mail: tahei@riken.jp
Homepage: http://www.riken.jp/lab-www/spectroscopy/en/index.html

Supporting information for this article is available on the WWW under http://www.angewandte.org or from the author.

in the electronic ground state. With the subsequent two ω_1 pulses, the fourth-order nonlinear polarization of $\omega_2-\omega_1+\omega_1+\omega_1=\omega_1+\omega_2$ is generated. We name this nonlinear process $\chi^{(4)}$ Raman, because the left two arrows and right three arrows correspond to the Stokes Raman and anti-Stokes hyper-Raman processes, respectively. The $\chi^{(4)}$ polarization creates signal light having the same photon energy and the same propagation direction as ESFG. Therefore, the $\chi^{(4)}$ signal is heterodyned with the $\chi^{(2)}$ ESFG signal that acts as a local oscillator. Because the $\chi^{(4)}$ signal is interface-specific and vibrationally resonance-enhanced, the heterodyne-detected $\chi^{(4)}$ Raman spectrum provides an interfacial vibrational spectrum when it is plotted as a function of $\omega_2-\omega_1$. We have already reported homodyne $\chi^{(4)}$ Raman spectroscopy, which measures $3\omega_1-\omega_2$ signals.[8] However, the present heterodyne $\chi^{(4)}$ Raman spectroscopy is advantageous, because of higher signal-to-noise ratio, easier experimental procedure, and no need for spectral-sensitivity correction. We note that the time-domain counterpart of the present frequency-domain method was demonstrated by several groups.[9–11] The advantage of the frequency-domain method is the much wider spectral range that can cover the whole fingerprint region, and no requirement for time-delay scan.

Figure 1d shows the ESFG spectrum of R800 adsorbed at the air/water interface. (Experimental details including fundamental characteristics of interfacial R800 are described in the Supporting Information.) The ω_1 pulse is at 795 nm, while the ω_2 pulse covers a wide range of 540–1200 nm. Under these conditions, the ESFG signal is enhanced by one- and two-photon double resonance with the electronic excited states of R800. The ESFG intensity in Figure 1d, I_d, is written as Equation (1).

$$I_d \propto |\chi^{(2)} E_1 E_2|^2 \quad (1)$$

E_1 and E_2 stand for the electric fields of the ω_1 and ω_2 pulses, respectively. With a ω_1 pulse energy 36 times larger than that for the spectrum in Figure 1d, we obtained the ESFG spectrum shown in Figure 1e. This spectrum shows proportionally higher ESFG intensity, as expected for the larger ω_1 pulse energy, but simultaneously it exhibits sharp features around 375 nm. These sharp features are ascribed to a higher order nonlinear effect induced by the larger ω_1 pulse energy, because they are absent in Figure 1d. The relevant higher order effect is the $\chi^{(4)}$ process that is diagrammatically represented in Figure 1c. The intensity I_e of the signal in Figure 1e is written as Equation (2).

$$I_e \propto |\chi^{(2)} E_1' E_2 + \chi^{(4)} E_1' E_1' E_1'^* E_2|^2 \quad (2)$$

Herein, E_1' represents the ω_1 electric field for the spectrum in Figure 1e (i.e., $|E_1'/E_1|^2=36$), and $E_1'^*$ the complex conjugate of E_1'. Equation (2) describes how $\chi^{(4)}$ is mixed with $\chi^{(2)}$ for optical heterodyne detection (see the Supporting Information).

In Figure 2, the $\chi^{(4)}$ contribution is compared with a bulk vibrational spectrum of R800 to confirm that the sharp downward bands are really due to vibrational resonances. Figure 2a shows the conventional spontaneous Raman spectrum of R800 powder. To show the $\chi^{(4)}$ contribution clearly, the following ratio of I_d to I_e was calculated [Eq. (3); the second order term of $\chi^{(4)}$ is neglected].

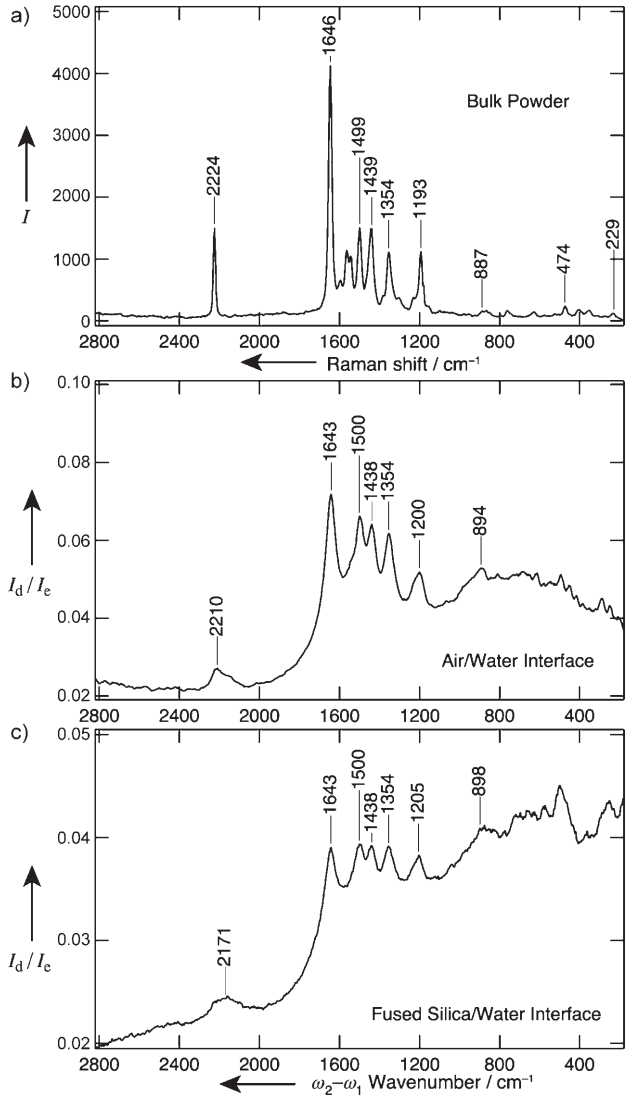

Figure 2. a) Spontaneous Raman spectrum of R800 powder. The spectral resolution was 22 cm^{-1}. See the Supporting Information for details. b) $\chi^{(4)}$ Raman spectrum of R800 at the air/water interface. c) $\chi^{(4)}$ Raman spectrum of R800 at the fused silica/water interface. For b) and c), the spectral resolution was 51 cm^{-1}.

$$I_d/I_e = |E_1/E_1'|^2(1-2|E_1'|^2\,\mathrm{Re}[\chi^{(2)}/\chi^{(4)}]) \quad (3)$$

Figure 2b plots the ratio I_d/I_e along the wavenumber axis of $\omega_2-\omega_1$. The peak positions in I_d/I_e are in very good agreement with those in the spontaneous Raman spectrum of the R800 powder (Figure 2a), which indicates that I_d/I_e undoubtedly represents the "$\chi^{(4)}$ Raman spectrum" of R800 at the air/water interface. (Exactly speaking, $\chi^{(4)}$ is just an ingredient of I_d/I_e, as shown in Equation (3), but we simply name I_d/I_e the $\chi^{(4)}$ Raman spectrum because the sharp features arise solely from $\chi^{(4)}$.) Figure 2c shows the $\chi^{(4)}$ Raman spectrum of R800 at a fused silica/water interface, which

was acquired in the same way as that for the air/water interface. Note that VSFG cannot be readily applied to this silica/water interface for the present wavenumber region because of the very strong IR absorption of water and fused silica glass.

The $\chi^{(4)}$ Raman spectrum at the air/water interface exhibits nearly the same peak positions as the Raman spectrum of the powder for the 800–1700 cm^{-1} region, but the C≡N stretching band around 2200 cm^{-1} shows a substantial red shift at the air/water interface. The $\chi^{(4)}$ Raman spectrum at the silica/water interface exhibits the same peak positions within ± 5 cm^{-1} as that at the air/water interface for the 800–1700 cm^{-1} region. However, the C≡N stretching band shows a further red shift at the silica/water interface compared with the air/water interface. These results indicate that the C≡N stretching frequency sensitively probes the difference in the molecular environment. Because the C≡N functional group is an H-bond acceptor, the C≡N stretching frequency reflects the surrounding H-bonding structure. The other vibrational bands in the region of 800–1700 cm^{-1} are ascribed to the vibrations of the xanthene ring structure of R800, and they are not very sensitive to the surrounding environment.

The C≡N bands of R800 in different environments are compared in Figure 3a. The C≡N peak position in bulk water and ethanol is 6–8 cm^{-1} higher than that of the powder. Because the powder provides an H-bond-free environment, it is concluded that the H-bonding interaction between R800 and water (or ethanol) induces the blue shift of the C≡N frequency in the bulk solution. It is well known that the C≡N band of nitrile compounds shows a blue shift in protic solvents compared with aprotic environments because of the H-bonding interaction.[12–16] In contrast, the C≡N peak position at the air/water interface is 14 cm^{-1} lower than that of the powder, and, remarkably, the peak position at the fused silica/water interface is 53 cm^{-1} lower. To the best of our knowledge, a red shift of the C≡N band in a bulk solvent has never been reported. The red shifts indicate a unique solute–solvent interaction that is specific to the interfaces.

Density functional theory (DFT) calculations provide key information about solute–solvent interactions that induce a frequency shift of the C≡N stretching vibration. As a model for R800 in bulk water, an R800 molecule solvated with 12 water molecules was calculated at the B3LYP/6-31 + G* level using Gaussian 03 (see the Supporting Information for details). The optimized structure of this R800-$(H_2O)_{12}$ model cluster is shown in Figure 3b. In this cluster, eight water molecules form an H-bonding network in the vicinity of the nitrile group, and the OH group of a water molecule is H-bonded linearly to the N atom. In this so-called σ-type H-bond, the lone-pair electrons of the N atom accept the H-bond.[17] The calculated C≡N frequency of the R800-$(H_2O)_{12}$ cluster is 2346.5 cm^{-1} (without any scaling), which is 9.8 cm^{-1} higher than the calculated frequency of R800 free of water. This confirms that the σ-type H-bond induces the blue shift of the C≡N frequency, which is in good qualitative agreement with a gas-phase spectroscopic study on benzonitrile clusters.[17] It is concluded that the R800-$(H_2O)_{12}$ cluster is a good model for R800 in the bulk solution.

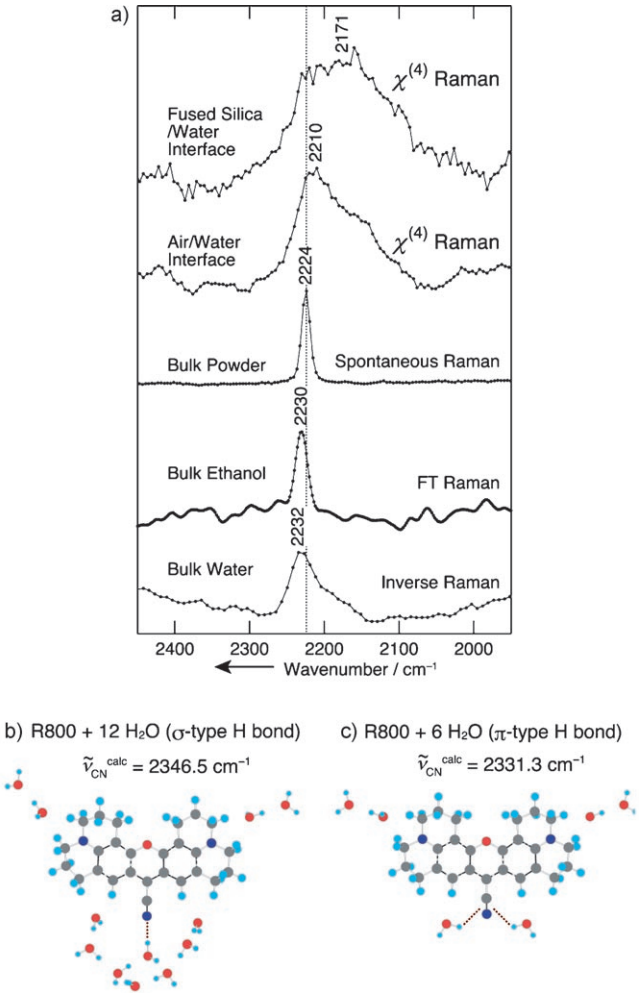

Figure 3. a) C≡N vibrational bands in various environments. The upper three spectra are the same data as in Figure 2, except that background subtraction was performed for the $\chi^{(4)}$ Raman spectra. The FT-Raman spectrum of R800 in bulk ethanol was measured with a spectral resolution of 16 cm^{-1}. The inverse Raman spectrum of R800 in bulk water was measured with a spectral resolution of 27 cm^{-1}. See the Supporting Information for details. b) Optimized structure of R800 with 12 water molecules. A water molecule is H-bonded to the nitrile N atom in the σ-type configuration. c) Optimized structure of R800 with six water molecules. Two water molecules are H-bonded to the C≡N bond in the π-type configuration.

The red shift of the C≡N frequency at the interfaces was reproduced in DFT calculations on a R800-$(H_2O)_6$ cluster, in which the number of water molecules around the nitrile group was reduced to two. Figure 3c shows the optimized structure of the R800-$(H_2O)_6$ cluster. The OH groups of the two water molecules are H-bonded nearly perpendicularly to the C≡N bond. This is known as a π-type H-bond, because the π electrons of the triple bond accept the H-bond.[17] According to the DFT calculations, the C≡N stretching frequency of the R800-$(H_2O)_6$ cluster is 2331.3 cm^{-1}, which is 5.4 cm^{-1} lower than that of free R800, and 15.2 cm^{-1} lower than that of the R800-$(H_2O)_{12}$ cluster. Experimentally, the red shift of the C≡N frequency from bulk water to the air/water interface is 22 cm^{-1}, which is close to the theoretically calculated

difference between the R800-$(H_2O)_{12}$ and R800-$(H_2O)_6$ clusters. The DFT calculations on the model clusters strongly indicate that the π-type H-bond is the origin of the red shift of the C≡N frequency that was found for R800 at the air/water interface.

The π-type H-bond between the C≡N group and water has been experimentally found only in the gas phase so far,[17–19] because a π-type H-bonded complex is formed only when the nitrile group is surrounded by a small number of water molecules. In bulk liquid phases, the nitrile group is inevitably surrounded by many water molecules, and this results in formation of a σ-type H bond. Because the present result shows that the π-type H-bonded complex exists at the air/water interface, it can be concluded that the C≡N group of R800 is located in a water-deficient local environment that effectively restricts the number of interacting water molecules to one or two. The orientation of R800 is expected to play a crucial role in realizing such a situation at the interface. From polarization second-harmonic generation (SHG) measurements (see the Supporting Information), the angle of the molecular long axis of R800 with respect to the air/water interface normal was determined to be $(61 \pm 2)°$. Although the orientation of the C≡N group could not be determined directly by the SHG measurements, it is likely that a water-deficient local environment of the C≡N group is realized if it points upward with the long axis kept at 61°. We note that this orientation is energetically favorable, because the positive charge on the xanthene ring is stabilized by water solvation. Obviously, such a situation is realized only at the interface, and in this sense, the π-type H-bonded complex of R800 and water is an interface-specific species.

The red shift of the C≡N band of R800 at the fused silica/water interface is much larger than that at the air/water interface. In fact, the red shift at the silica/water interface is as large as that reported for metal nitrile complexes in which the C≡N bond is coordinated to a metal atom in the π-type configuration.[20] The large red shift of metal nitrile complexes is attributable to the strong coordinative-bonding interaction. A recent VSFG study on silica/water interfaces indicated a wide distribution of pK_a values for the OH groups of the silica surface.[21] It was shown that a significant number of surface sites were deprotonated even at pH as low as 1.5. Because of such strong proton-donating ability, it is expected that the OH groups of the silica surface can undergo stronger H-bonding interaction with the C≡N group of R800 than with the OH group of water. Thus, it is likely that the large red shift of the C≡N frequency at the fused silica/water interface is due to strong π-type H-bonding interaction between the C≡N group and the OH groups of the silica surface. The large red shift does not seem to be simply ascribable to a specific orientation at the silica/water interface, because the angle of the molecular long axis of R800 with respect to the silica/water interface normal was determined to be $64 \pm 10°$ by SHG polarization measurements, which is very close to the angle at the air/water interface.

Received: April 12, 2007
Revised: July 13, 2007
Published online: August 23, 2007

Keywords: density functional calculations · hydrogen bonds · interfaces · nonlinear optics · vibrational spectroscopy

[1] C. T. Williams, D. A. Beattie, *Surf. Sci.* **2002**, *500*, 545.
[2] C. D. Bain, *J. Chem. Soc. Faraday Trans.* **1995**, *91*, 1281.
[3] A. M. Briggs, M. S. Johal, P. B. Davies, *Langmuir* **1999**, *15*, 1817.
[4] P. B. Miranda, Y. R. Shen, *J. Phys. Chem. B* **1999**, *103*, 3292.
[5] G. L. Richmond, *Chem. Rev.* **2002**, *102*, 2693.
[6] Z. Chen, Y. R. Shen, G. A. Somorjai, *Annu. Rev. Phys. Chem.* **2002**, *53*, 437.
[7] S. Yamaguchi, T. Tahara, *J. Phys. Chem. B* **2004**, *108*, 19079; S. Yamaguchi, T. Tahara, *J. Chem. Phys.* **2006**, *125*, 194711.
[8] S. Yamaguchi, T. Tahara, *J. Phys. Chem. B* **2005**, *109*, 24211.
[9] Y. M. Chang, L. Xu, H. W. K. Tom, *Phys. Rev. Lett.* **1997**, *78*, 4649.
[10] K. Watanabe, N. Takagi, Y. Matsumoto, *Chem. Phys. Lett.* **2002**, *366*, 606; K. Watanabe, N. Takagi, Y. Matsumoto, *Phys. Rev. Lett.* **2004**, *92*, 057401.
[11] S. Fujiyoshi, T. Ishibashi, H. Onishi, *J. Phys. Chem. B* **2004**, *108*, 10636; S. Fujiyoshi, T. Ishibashi, H. Onishi, *J. Phys. Chem. B* **2005**, *109*, 8557; S. Fujiyoshi, T. Ishibashi, H. Onishi, *J. Phys. Chem. B* **2006**, *110*, 9571.
[12] H. Abramczyk, W. Reimschussel, *Chem. Phys.* **1985**, *100*, 243.
[13] W. O. George, B. F. Jones, R. Lewis, J. M. Price, *Phys. Chem. Chem. Phys.* **2000**, *2*, 4910.
[14] E. S. Kryachko, M. T. Nguyen, *J. Phys. Chem. A* **2002**, *106*, 4267.
[15] P. Raghuvansh (nee Bhriguvansh), S. K. Srivastava, R. K. Singh, B. P. Asthana, W. Kiefer, *Phys. Chem. Chem. Phys.* **2004**, *6*, 531.
[16] J. M. Alía, H. G. M. Edwards, *J. Phys. Chem. A* **2005**, *109*, 7977.
[17] S. Ishikawa, T. Ebata, N. Mikami, *J. Chem. Phys.* **1999**, *110*, 9504.
[18] K. Egashira, Y. Ohshima, O. Kajimoto, *Chem. Phys. Lett.* **2001**, *334*, 285.
[19] K. Sakota, N. Yamamoto, K. Ohashi, M. Saeki, S. Ishiuchi, M. Sakai, M. Fujii, H. Sekiya, *Chem. Phys.* **2002**, *283*, 209.
[20] B. N. Storhoff, J. Huntley C. Lewis, *Coord. Chem. Rev.* **1977**, *23*, 1.
[21] V. Ostroverkhov, G. A. Waychunas, Y. R. Shen, *Phys. Rev. Lett.* **2005**, *94*, 046102.

